



## Morphometric Analysis of Mount Ararat (Eastern Anatolia, Türkiye)

Vedat Avci<sup>1,\*</sup>, Murat Sunkar<sup>2</sup>, Ahmet Toprak<sup>2</sup>

<sup>1</sup>Department of Geography, Faculty of Arts and Science, Bingöl University, Bingöl, Türkiye

<sup>2</sup>Department of Geography, Faculty of Humanities and Social Sciences, Fırat University, Elazığ, Türkiye

### Article History

Received: 18.12.2021  
Accepted: 10.03.2022  
Published: 25.09.2022

### Research Article

**Abstract** – In this study, the morphometric characteristics of Mount Ararat which is a strato-volcano are analyzed. Türkiye's highest Mountain, Mount Ararat, is located in Eastern Anatolia. The Mountain takes the shape of two major volcanic cones after 2500 m height; these volcanic cones are named Greater Mount Ararat (5137 m) and Little Mount Ararat (3896 m). In this study, relief morphometry, basin morphometry, and drainage characteristics are morphometrically analyzed with Geographic Information Systems (GIS) using 10x10 m resolution Digital Elevation Model (DEM). According to the analysis results, there is an increase in the elevation on the high and steep slopes of the main cone and the slope values increase up to 56° in some locations towards the summit. On the other hand, according to the aspect analyses, 19.9% of slope faces are north-east direction, 14.7% of the slopes are north-direction, 9.4% are northwest, 9.8% are west, 10.7% are southeast, and 16.4% of the slopes are east direction. These results support the fact that Mount Ararat extends in NW-SE direction and is formed on the basis of a fault line in this direction. According to the grouping made by the altitude ranges analysis, the decrease in the rate of elevation belts starting from the slopes of the mountain towards the top confirms the structure of volcanic cone. Elevation differences in relative relief analyses range between 0 and 1141 m and this value increases to 1141 m on the slopes surrounding the summit. The cone structure of Mount Ararat was prominent in transverse and longitudinal profile analyses.

**Keywords** – Eastern anatolia, geographic information systems, mount ararat, morphometric analysis, strato-volcano

### 1. Introduction

Mount Ararat is at the intersection of the borders between Türkiye, Armenia, Azerbaijan, and Iran. The volcanic mountain is formed on a circular base with a diameter of 30-35 km. Greater Mount Ararat is Türkiye's highest mountain with 5137 m elevation. Mount Ararat is a (strato-volcano) volcano that was formed as a result of the multi-period and accumulation of lava and tuffs on one another (Figure 1). The Cone-shape and high and steep slopes of the Mountain are the results of non-flowing lava that cools and solidifies quickly. The volcanic mass, which is basically formed as a single body, rises as two separate volcanic cones after 2500 m. The cone in the west is Greater Mount Ararat (5137 m) while the cone in the east is Little Mount Ararat (3896 m). Greater Mount Ararat has a relative elevation difference of 4300 m compared to Iğdır plain, which is located in the North, and more than 3000 m compared to Doğubayazıt located in the south (Figure 2).

Increased with altitude, the degree of slope on the Mount Ararat varies between 0° and 56°. There is a distances of 10 km between the summits of Greater Mount Ararat and Little Mount Ararat and they are similar in terms of structure as they were formed in the same period (Atalay, 2017; Kaya, 2017; Şahin, 2011). Mount Ararat, which is a multi-period strato-volcano, consists of acidic lava flows, agglomerates, and tuffs. As a result of the Quaternary volcanism, approximately 3x10<sup>12</sup> tons of volcanic material surfaced (Türkünal, 1980). Agglomerate, volcanic breccia, obsidian, and ashes are common materials on the bases of the cones while the last surfaced materials are tuffs. It is assumed that the cones were formed in two possible

<sup>1</sup> [vavci@bingol.edu.tr](mailto:vavci@bingol.edu.tr)

<sup>2</sup> [sunkarmurat@gmail.com](mailto:sunkarmurat@gmail.com)

<sup>3</sup> [atoprak@firat.edu.tr](mailto:atoprak@firat.edu.tr)

\*Corresponding Author

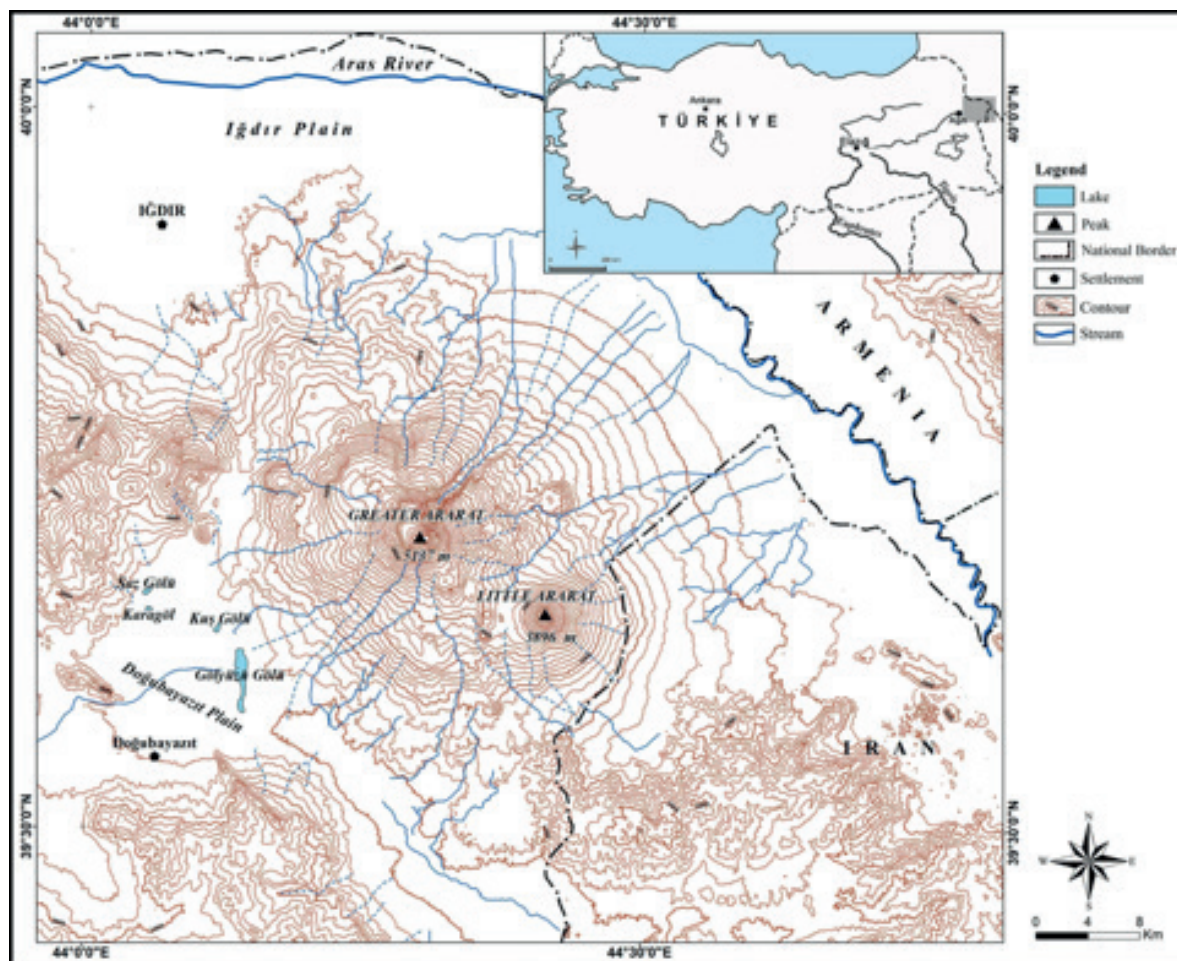


Figure 1. Location map of Mount Ararat.

phases according to their morphological status. According to that assumption, the andesitic structure of the two cones was formed in the Early Quaternary in the first phase while young lava flows and parasitic cones were formed in the Late Quaternary in the second phase (Blumenthal, 1958). Apart from this view, (Güner & Şaroğlu, 1987) state that Mount Ararat consists of 11 different stages (Türkecan, 2017).

Quaternary basalt, andesite, and pyroclastic rocks cover a large surface on Mount Ararat (Şenel & Ercan, 2002). The alluvial materials were carried by the rivers originating from the summit of the Greater and the Little Ararat and created thick deposits in the north-eastern fans (Figure 3). The permanent snow line on Mount Ararat starts at 4000 m and after this elevation, a part covering 1000 m is in the permanent snow limit. The summit of the mountain is covered with a wide ice cap glacier (Erinç, 1953). Besides being the highest summit of Türkiye, Mount Ararat has a current 10 km<sup>2</sup> ice cap (Arkel, 1973; Imhof, 1956). According to (Blumenthal, 1956, 1958) 11 glacial tongues hanging from the ice cap with lengths varying from 1 to 2,5 km reach to 4200 m on the southern slopes and 3900 m on the northern slopes (Çiner, 2003). Geomorphology studies on the whole mountain haven't been conducted because of the reasons such as the height of Mount Ararat, the area it occupies, transportation and security. However, the glaciers on Mount Ararat have attracted the attention of many researchers for a long time and there are many types of research about glaciers (Arkel, 1973; Blumenthal, 1956, 1958; Çiner, 2003; Erinç, 1953; Imhof, 1956; Sarıkaya, 2012; Azzoni et al., 2017). According to the title of the article prepared by Azzoni et al., (2017) it is thought that the geomorphology of Mount Ararat is investigated. However, by the content of the article it is understood that the glaciers on the mount are studied using satellite images. Apart from the glaciers, catastrophic events having occurred in Ahora Gorge on the mount is evaluated (Azzoni et al., 2019). In the literature, quantitative analyses reflecting its topographic and geomorphological features have not been performed on Mount Ararat.

As it is difficult for today to study the geomorphology of Mount Ararat due to geographical conditions and security issues, the goal of this study is to make morphometric analyses showing geomorphologic features.

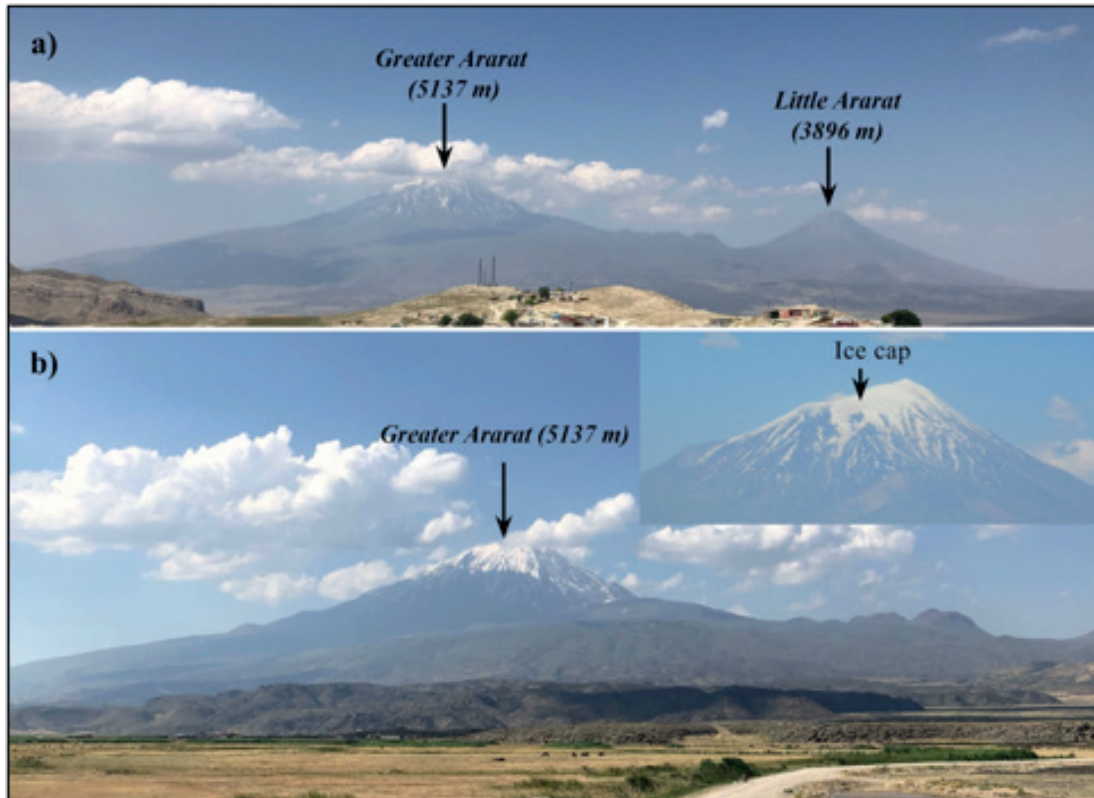


Figure 2. In Eastern Anatolia, Mount Ararat (Ağrı) is located at the intersection of the border between Türkiye and Armenia, Azerbaijan and Iran. The Greater and Little Mount Ararat (a) and glaciers on the Greater Mount Ararat (b).

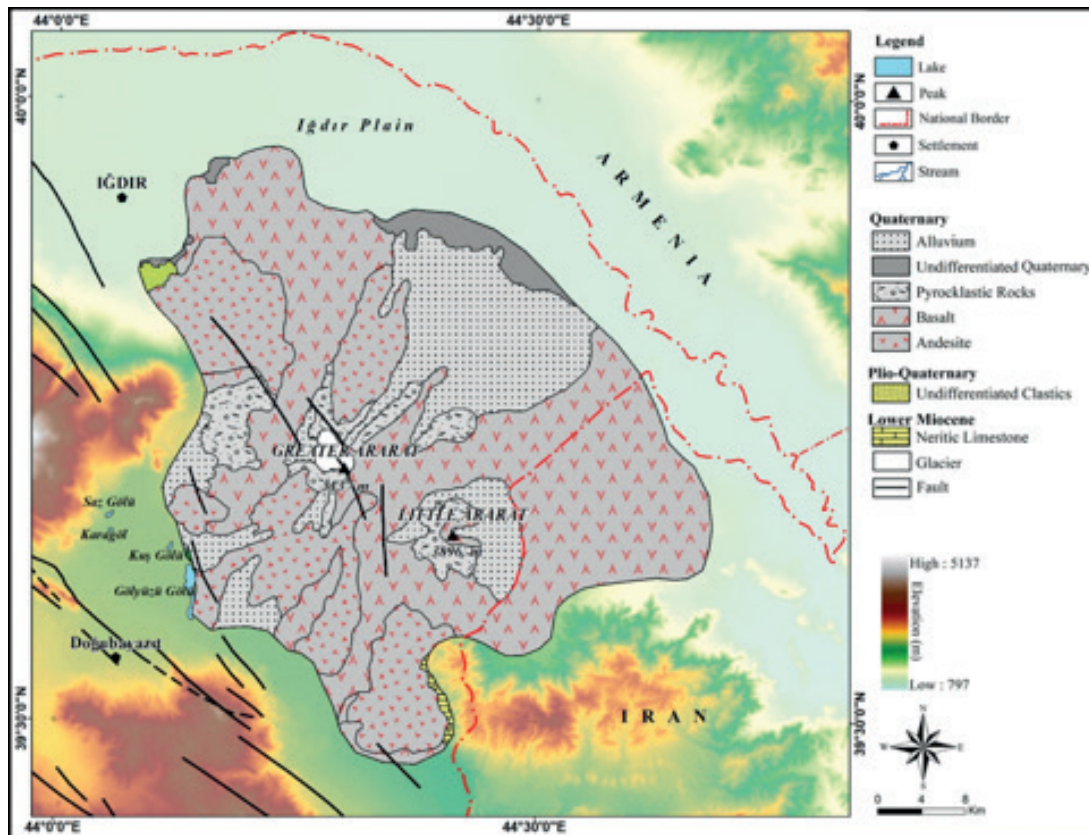


Figure 3. Geological map of Mount Ararat (The figure is drawn on the basis of MTA 1/500.000 scale Geological Map of Türkiye, Van Sheet by (Şenel & Ercan, 2002).

Morphometry is defined as the analysis by using geographic information technologies for the purpose of obtaining data about geomorphologic units on the basis of the altitude values of that region (DEM-Digital Elevation Model). The data obtained with morphometric analyses can provide rapid and reliable information about the drainage development in an area, influence level of the structure and lithology on this development and distribution and properties of structure (Keller, & Pinter, 2002). Because of this advantage of morphometric analysis, the method has been preferred in many recent studies on the issue (Avcı & Sunkar, 2015, 2018; Avcı, Sunkar, & Toprak, 2018; Erginal & Cürebal, 2007; Özşahin, 2015; Topuz & Karabulut, 2016).

## 2. Materials and Methods

In order to analyze the geomorphological features of Mount Ararat, this article has been prepared using also indices in addition to oral presentation. On the basis of lithology and morphology, the border of the mountain has been determined according to topography, geological maps and satellite images. Analyses, which reveal the cone- or shield-shaped structure of volcanic mountains within these boundaries, have been used. In order to determine the morphometric properties of Mount Ararat, 15 morphometric analyses were performed for analysing relief morphometry, basin morphometry and drainage characteristics (Table 1).

Table 1

Formulas and results used in morphometric analyses of Mount Ararat

No	Morphometric Parameter	Formula	Reference	Result	Unit
1	Stream Order	Hierarchical Rank	(Strahler, 1952a)	1 to 6	Dimensionless
2	1 <sup>st</sup> Order Stream (Suf)	Suf = N1, N1 = 1 <sup>st</sup> Order Stream	(Strahler, 1952a)	14.483	Dimensionless
3	Stream Number (Nu)	Nu = N1 + N2 ..... Nn, N1, N2= Number of the streams.	(Horton, 1945)	19.041	Dimensionless
4	Stream Length (Lu)	Lu = L1 + L2 ..... Ln L1, L2= Length of the stream.	(Horton, 1945)	5046,8	km
5	Stream Length Ratio (Lur)	Lur = L1/Lu + 1 Lu= Stream Length (km)	(Horton, 1945)	0,49-0,62	Dimensionless
6	Basin Area (km <sup>2</sup> )	It was calculated with calculate geometry tool.	(Schumm, 1956)	1662	km <sup>2</sup>
7	Drainage Density (Dd)	Dd = Lu/A Lu= Total drainage length, A= Area.	(Horton, 1932)	3,7	km/km <sup>2</sup>
8	Hypsometric Curve	y = h/H, x = a/A, y= Relative Height, x= Relative Area	(Strahler, 1952b)	Concave curve	Dimensionless
9	Hypsometric Integral	Hi = (Hmean - Hmin)/(Hmax - Hmin), Hmean= Mean elevation (m), Hmin= Minimum elevation (m), Hmax= Maximum elevation (m).	(Strahler, 1952b)	0,28	Dimensionless
10	Aspect	Derives aspect from a raster surface. The aspect identifies the downslope direction of the maximum rate of change in value from each cell to its neighbors (Arcgis Desktop Help, 2022).		151,69	(o)

Table 1

Formulas and results used in morphometric analyses of Mount Ararat (Continued)

No	Morphometric Parameter	Formula	Reference	Result	Unit
11	Slope Analysis	Identifies the slope (gradient, or rate of maximum change in z-value) from each cell of a raster surface ( <u>Arcgis Desktop Help, 2022</u> )	( <u>Rich, 1916</u> )	0°-56°	(°)
12	Relative Relief	$Rr = H - h$ , H= Maximum elevation (m), h= Minimum elevation (m).	( <u>Smith, 1950</u> )	1141	m
13	Topographic Position Index	$Z = \frac{1}{NR} \sum ieRZi$ calculates the difference between the height (z) of point and mean height (m). The Radius is R.	( <u>Jenness, 2006</u> )	-18,2-25,1	Dimensionless
14	Topographic Curvature Analysis	$C = Z_{xx}^2 + Z_{xy}^2 + Z_{yy}^2$ Z= Elevation C= Curvature	( <u>Wilson and Gallant, 2000</u> )	-21,36-24,52	Dimensionless
15	Terrain Ruggedness Index	If each square represents a grid cell on a digital elevation model then, $TRI = Y[\sum(x_{ij} - x_{00})^2]^{1/2}$ where $x_{ij}$ elevation of each neighbor cell to cell (0,0) ( <u>Riley, DeGloria, &amp; Elliot, 1999</u> )	( <u>Riley, DeGloria, &amp; Elliot, 1999</u> )	0-2,5	Dimensionless

The DEM data used in these analyses have been created using 1/25000 scale topography maps of General Directorate Mapping (GDM, 2004) and Alos Palsar DEM data (ASF, 2019). DEM created from GDM and Also Palsar data have been combined through Data Management-Raster-Mosaic to New Raster module in the ArcGIS environment. All data in the study have been produced in the UTM WGS 84 Zone 38 projection system. Raster data have been reclassified using Reclassify tool. These reclassified layers have been converted to polygons through Conversion-Raster to Polygon tool. With this process, the area and ratio of the layer sub-groups have been determined. SAGA GIS software was used to obtain DEM data and Topographic Position Index and Terrain Ruggedness Index Maps were created accordingly. The data created by SAGA GIS were saved with File-Grid-Export tool in the file format to be used in ArcMap environment. The study area was divided into the sections of 1 km<sup>2</sup> grid; relative elevation differences of these grids were calculated by using zonal statistics which show the difference between the highest and the lowest points. On the basis of this difference, a relative relief map was created by using the Inverse Distance Weighted (IDW) method. The IDW method, which is one of the interpolation methods, consists of a calculation based on a logic whose value effect decreases as the distance of control points used in interpolation to the target point increases (Turoğlu, 2011). On the other hand, transverse and longitudinal profile series of Mount Ararat in the NE-SW and NW-SE directions were drawn.

### 3. Results and Discussion

#### 3.1. Profile Analyses

Topographic profiles are one of the most reliable tools used for accurate description and interpretation of landforms (Erol, 1993). The zigzag shape in a prepared profile shows that the topography in that area is rugged and has been split dissected too much (Bilgin, 2013). Profiles that are drawn for defining and bordering a morphological unit accurately provide highly reliable data in determining the processes through which the shapes are formed. It is usually possible to define topography maps and undefined ground patterns in field studies through these carefully drawn profiles. For this reason, profile analyses, which are under estimated today, are considered as one of the first issues that should be evaluated in geomorphology and

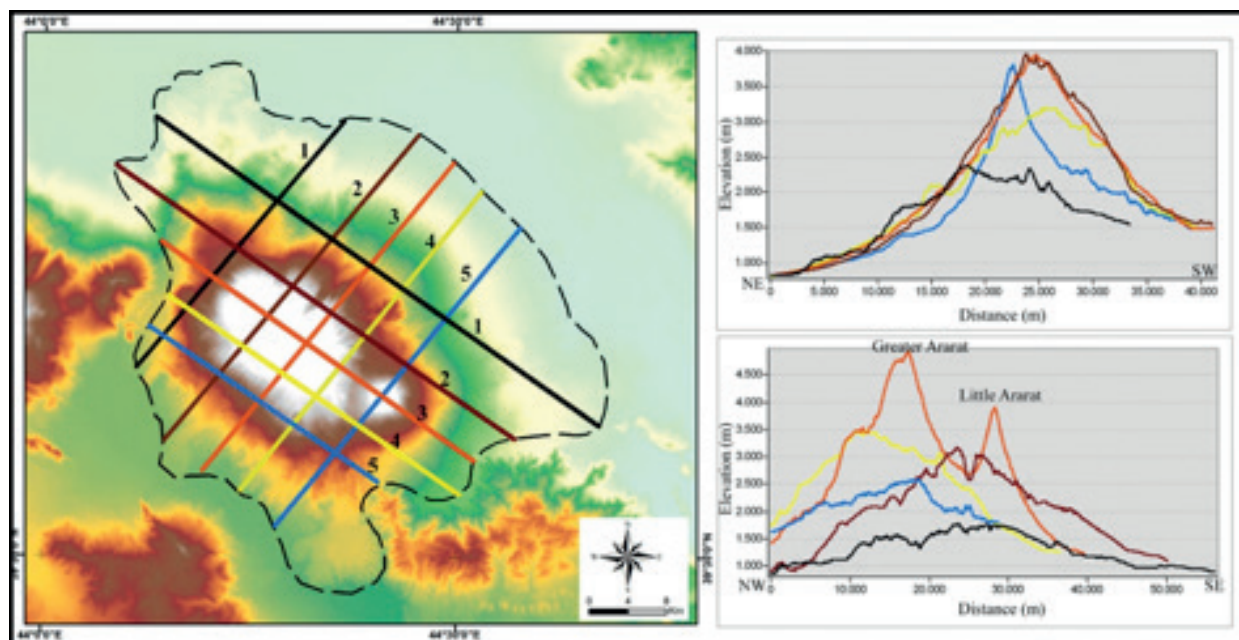


Figure 4. NW-SE and NE-SW directions profile series of Mount Ararat.

morphometry studies. In order to determine the morphological features of Mount Ararat, NW-SE and NE-SW profiles were constructed (Figure 4).

Despite its massive structure, Mount Ararat is made of two high summits. The presence of a smaller summit on the east of the main summit suggests that the mountain extends in the NW-SE direction. In fact, the diameter of the mountain in this direction is higher than that of the other direction. According to the NW-SE direction profiles, the Greater Ararat and Little Ararat cones start after the 2000-2500 m elevation range (Figure 4). On the other hand, according to the transverse and longitudinal profile series, there is a greater elevation difference between the mountain foot and the summit. Cone shape is very prominent in both profile series and the slopes start to incline after 2500 m elevation. It is also determined that the mountain rises on a wide base between 2000-1000 m elevation range.

### 3.2. Altitude Range Analysis

The altitude range analysis in morphometric analyses is used in the interpretation of topography. In this analysis, the Digital Elevation Model (DEM) is used as the basis. According to the classification, the elevation in the specifically limited area varies between 797 m and 5137 m (Figure 5). The volcanites of Mount Ararat start after 1000 m elevation in İğdir Plain and 1500 m elevation in Doğubayazıt Plain. The base is characterized by lava flows up to 2000 m and takes a typical cone shape after this elevation. There is a steady altitude increase between 2000-3000 m while the altitude increases at much shorter intervals after 3000 m. The areas below the altitude ranges of 2000-3000 m constitute the lower slope of the mountain while the upper areas constitute the cone. The area in this elevation range corresponds to the lower slope of the cone while the areas above this elevation are considered the summit of the Mountain.

DEM data in the studied area are divided into 18 classes; the size of each class is 250 m. In this classification, the area covered by the 797-1000 m altitude range covers the widest area when compared to the other ranges (Figure 6). It is determined that the young lava flows surfaced in the last period of the Mountain spread over İğdir Plain; this process is one of the reasons that contributed to the width of this area. The areas on 1000-1250 m altitude range correspond to the lava flows in İğdir Plain while they correspond to the plain base in Doğubayazıt Plain. The 1500-1750 m altitude range, which is the second widest area, corresponds to the low volcanic plateaus around the mountain. The plateaus at this step are the volcanic terrain formed by the spread of lava flows.

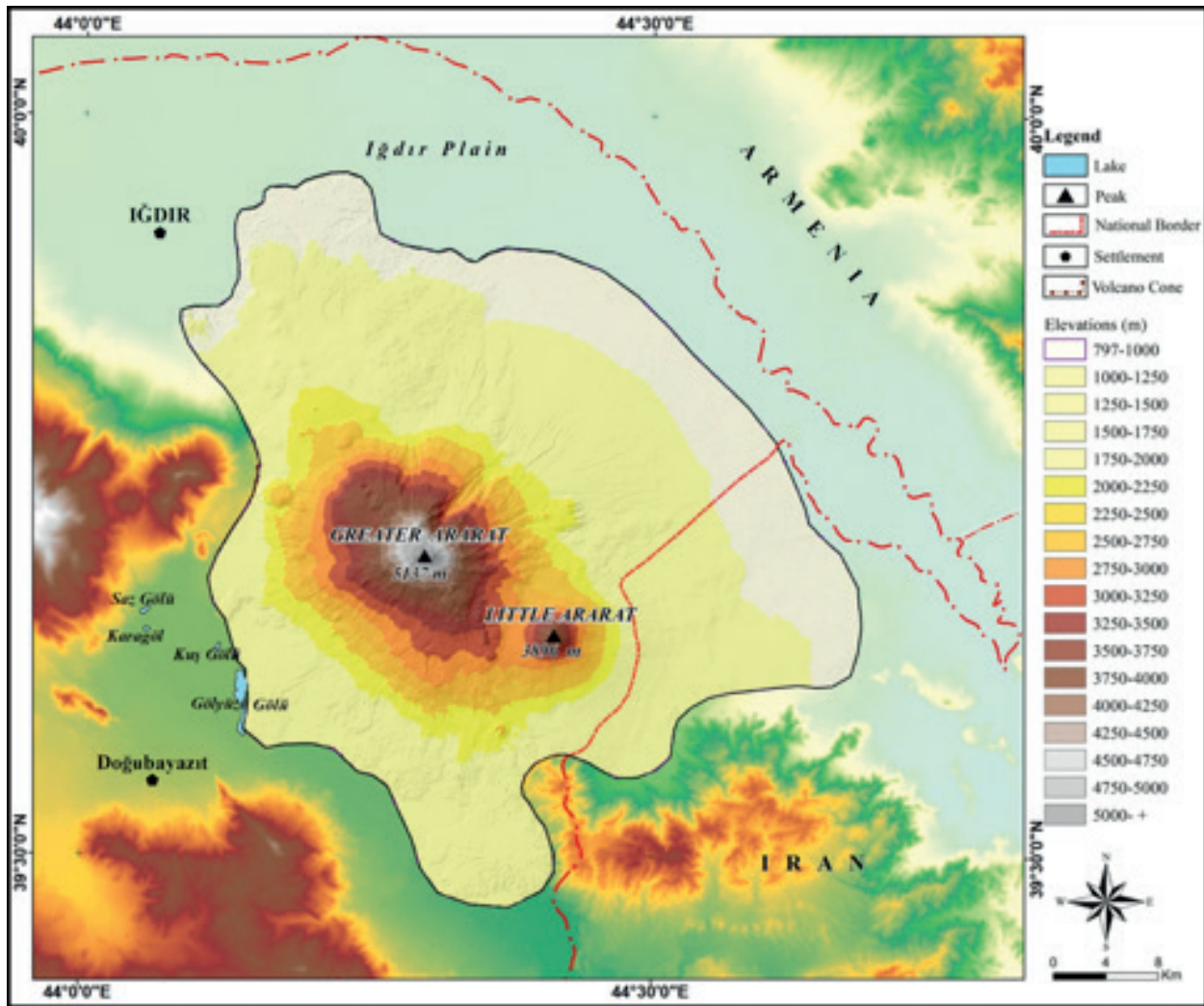


Figure 5. Altitude ranges map of Mount Ararat

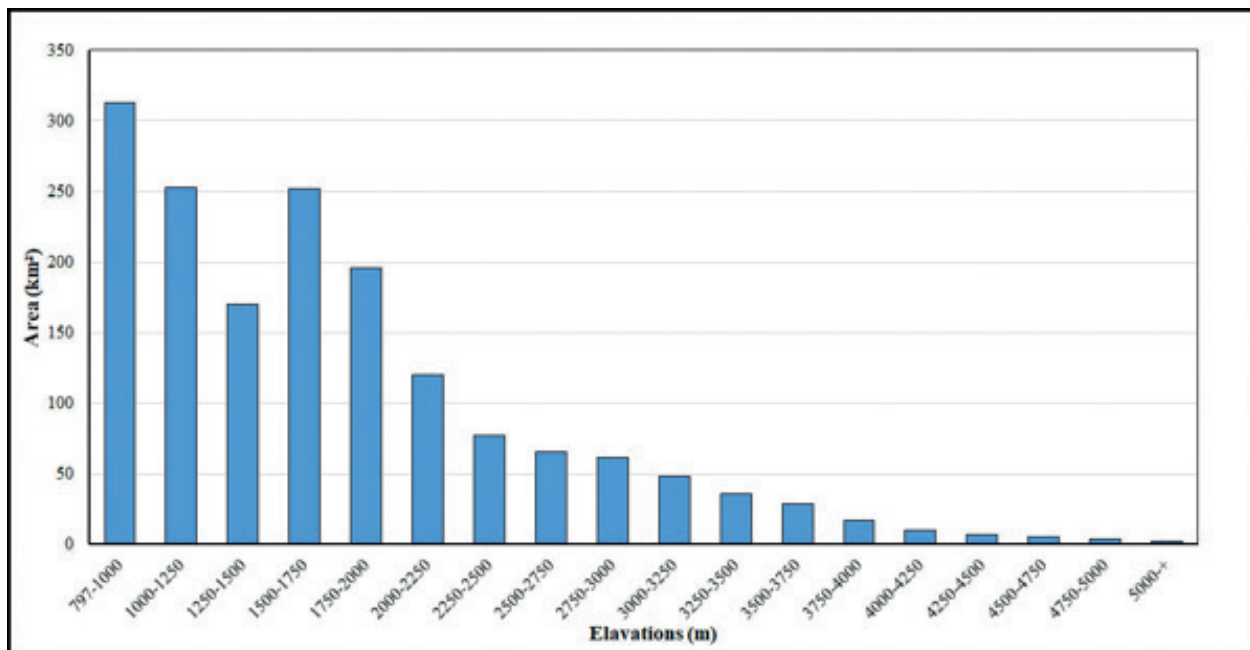


Figure 6. Mount Ararat altitude ranges areal distribution.

The altitude ranges between 797-1500 m have an approximate ratio of 44% in the study area according to the proportional distribution of the altitude ranges. The ranges between 1500-1750 m have a 15% ratio, 1750-2000 m have a 12% ratio, 2000-2250 m have a 7% ratio, 2250-2500 m have a 5% ratio, 2500-2750 m 4%, 2750-3000 m 4%, 3000-3250 m 3%, 3250-3500 m 3%, 3500-3750 m 2% and the ranges between 3750-4000 m have a 1% ratio in the whole area (Figure 7).

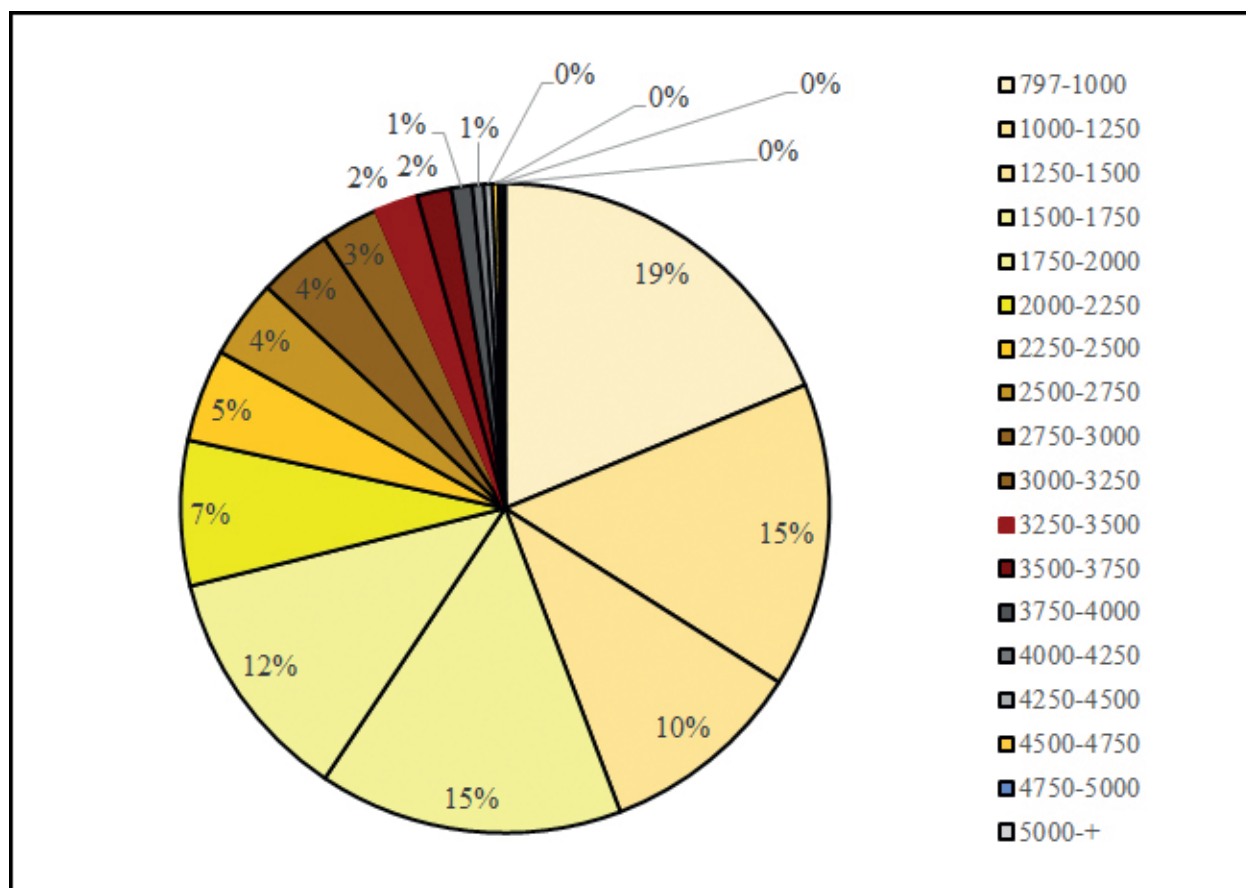


Figure 7. Mount Ararat altitude ranges proportional distribution.

According to the results of the analysis, the rate of the areas with an altitude below 2000 m. in the Mountain is 71% while the areas above this altitude correspond to 29 % of the Mountain. According to the results of this analysis, the areas covered by the altitude ranges surrounding the mountain proportionally decrease towards the summit. This fact confirms that the mountain is morphologically in the form of a volcanic cone.

### 3.3. Slope Analysis

The most important analysis that reveals the character of topography is slope analysis. The slope values of Mount Ararat vary between 0-56°. It is observed that the slope values generally increase in line with the increase in volcanic cone elevation on the slopes, which generally becomes apparent after 2500 m. The slope towards the summit reaches 56° in the areas over 3500-4000 m elevations (Figure 8). The dominant process that shapes the topography, breaks it up in different proportions, shapes slopes, and ridges which are formed in different directions and causes different slope values is the fluvial processes (Ardel, 1968). However, the effects of volcanic activity and glacial formation are also significant in the formation of a high slope at the summits of the Mountain. There are high slope values in stream valleys located on cone slopes in areas lower than 4000 m. Although the slope increases in line with the increase in elevation, slope values decrease towards the lower slope of the cone. The high inclination difference between the lower slope of the volcanic cone and the summit reflects the typical characteristics of the volcanic cones (Avci et al., 2018).

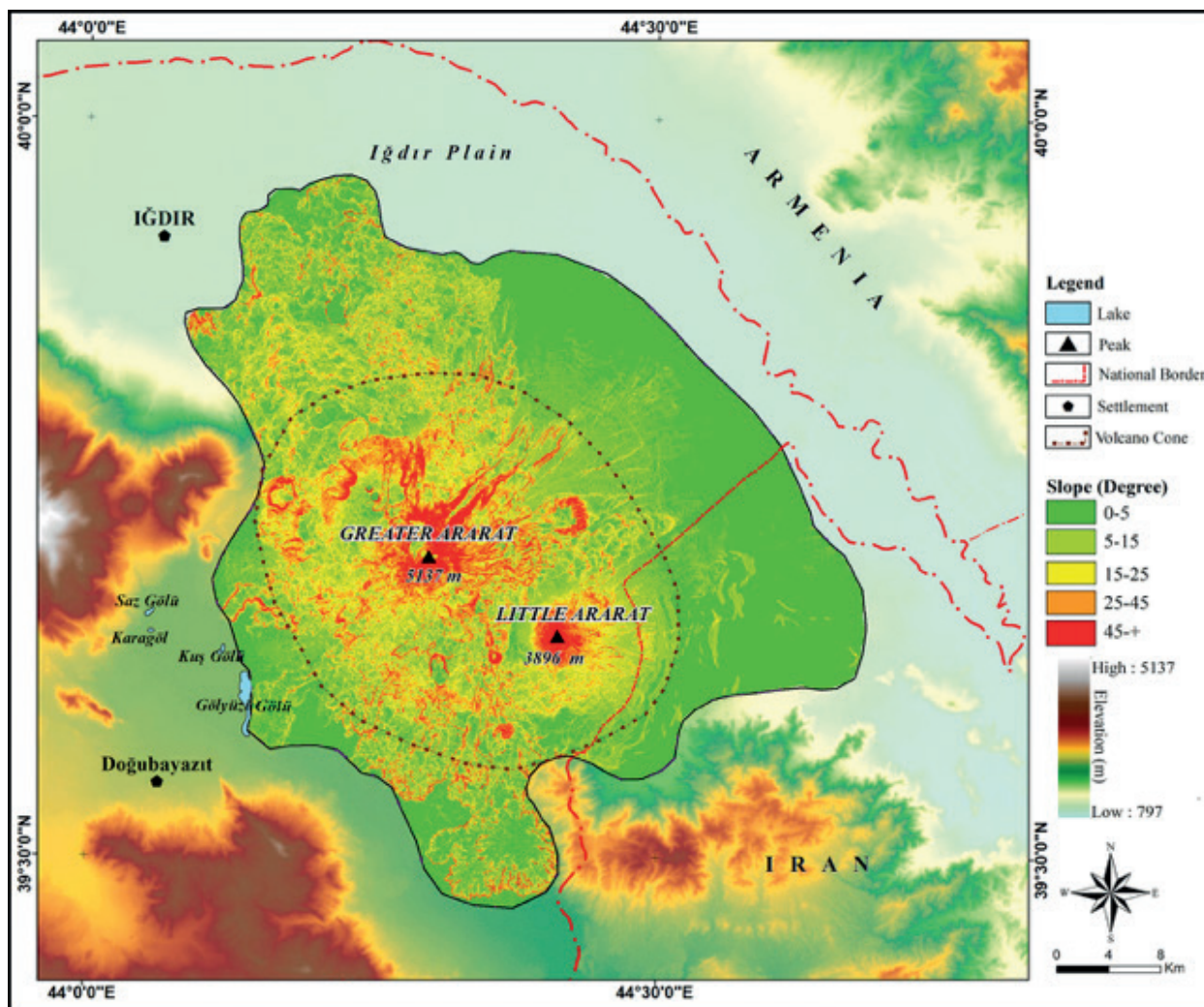


Figure 8. Slope map of Mount Ararat.

According to the slope map of Mount Ararat, there are important differences between the Eastern and Western slopes of the Mountain. The slope values of the west-facing slopes are higher than the East. Increased glacial activity on the East and North-East slopes supported the formation of the valley on these slopes. Thus, the incline in the slopes eroded by glaciers and rivers increased. Apart from this formation, young lava eruptions on the slopes facing northwest and southeast caused the slope to be partially low. When the slope values of Greater Ararat and Little Ararat are compared, it can be seen that the slope of the Mount Ararat regularly increases from the slopes of the cone to the summit. The inclination towards the summit is very high as the cone of Little Mount Ararat is younger and less eroded than the Greater Mount Ararat. On the other hand, as Greater Mount Ararat is older and higher than Little Mount Ararat, the slopes around the summit are eroded by glaciers and streams. Because of this process, slope values around the summit of Greater Mount Ararat are relatively low when compared to Little Mount Ararat. According to the reclassified slope map, nearly half of the researched area, whose slope level varies between 0 and 5°, constitutes 42% of Mount Ararat. Mountainside and the ranges in the mountainsides of Mount Ararat aren't included in the research field; this is why areas with low inclination cover a wide area. On the other hand, the very same data indicates that the mountain starts on a very wide and flat base. The areal and proportional change in slope groups from low to high reflects the typical characteristics of the volcanic cone (Figure 9).

The ratio of the areas in the 0-5° slope group in the limited (study) area is 42%. Areas with a slope between 5-15° are 25%, areas with a slope between 15-25° are 17%, and areas with a slope between 25-45° are 11%

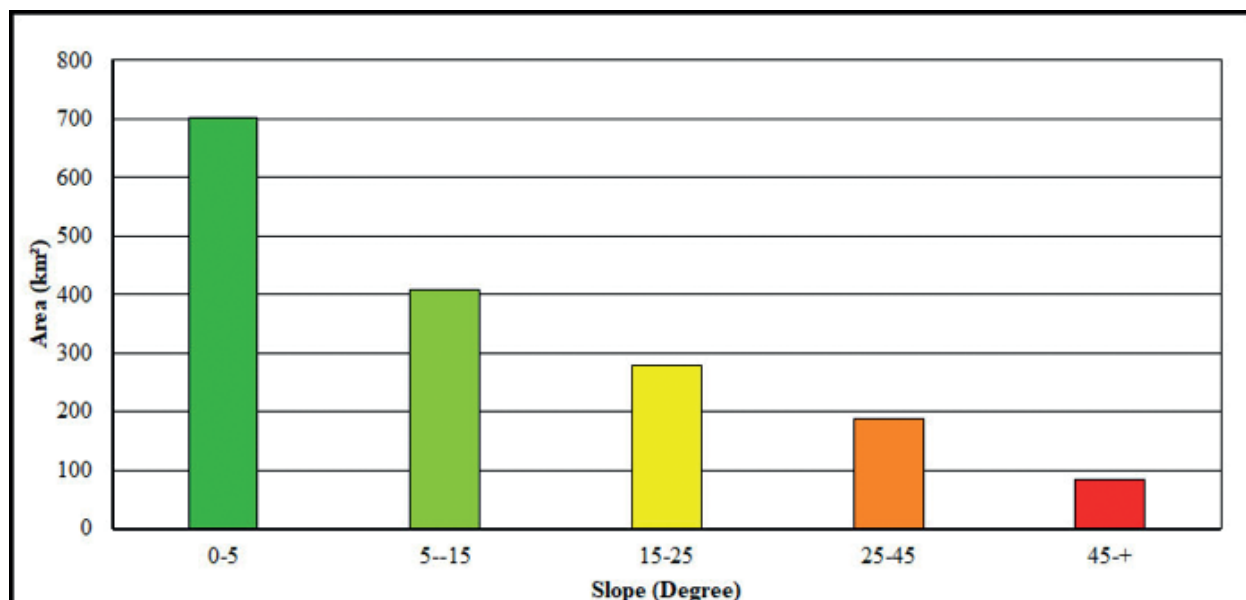


Figure 9. Areal distribution of the slope on Mount Ararat.

of the complete study area (Figure 10). The relative distribution of the slope groups gradually decreases approximately one degree in each group. The volcanic cone is characterized by this decrease; 5% of the slope groups have 45° and higher slope ratio.

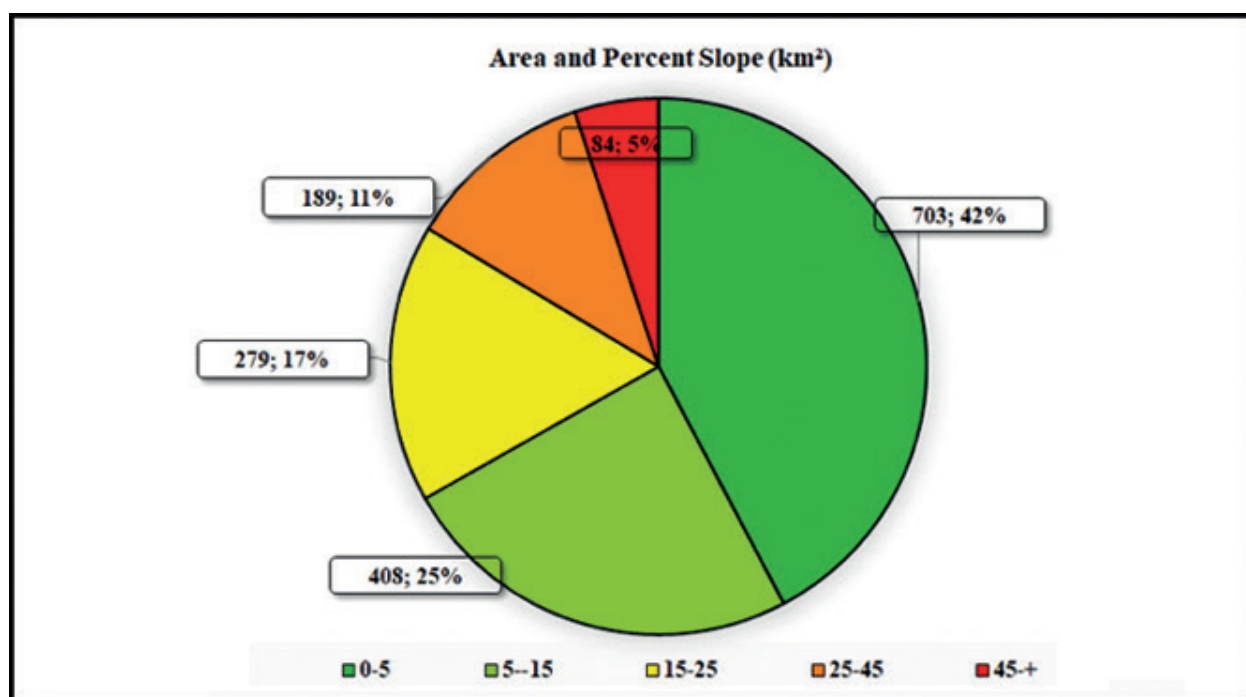


Figure 10. Proportional distribution of the slope in Mount Ararat

According to the slope analyses, the spatial and proportional distributions of the slope in Mount Ararat reflect the characteristics of volcanic cones. The wide and low slopes around the Mountain are dominant up to 2000 m altitude; there is a slow increase in the slope between 2000 m and 3000 m while there is a rapid slope increase after 3000 m towards the summit. The parasite cones on the main volcanic cone and the lava exit points in different areas led to the formation of different slope features on the greater cone. This is clearly observed on the northwest and southeast slopes of the Mountain.

### 3.4. Aspect Analysis

Aspect can be effective and guiding on environmental features in an area such as sunshine duration, sunshine intensity, humidity, rainfall, and wind, which are some of the climatic elements (Wilson & Gallant, 2000). According to the aspect map, the slopes facing north-northeast and south-southeast cover more areal and proportional areas (Figure 11). This partial difference shows that Mount Ararat extends in the direction of NW-SE. This result is also confirmed when aspect features are compared with the profiles. The reclassified aspect map is converted from raster format to vector format and the area covered by each aspect group is determined. According to the aspect map, the northeast slopes cover 1/5 of the study area. According to the aspect map, the ratio of flat areas is 1.6%, the ratio of the northern slopes is 14.7%, the ratio of the northeast slopes is 19.9%, the ratio of the eastern slopes is 16.4%, the ratio of the southeast slopes is 10.7%, the ratio of the south slopes is 8.7%, the ratio of the southwest slopes is 8.7% the ratio of the western slopes is 9.8% and the ratio of the northwest slopes is 9.4% (Table 2). While the total ratio of the northern slopes is 44%, the ratio of the southern slopes is 28.1% (Figure 12). This distribution shows that the mountain extends in the direction of NW-SE.

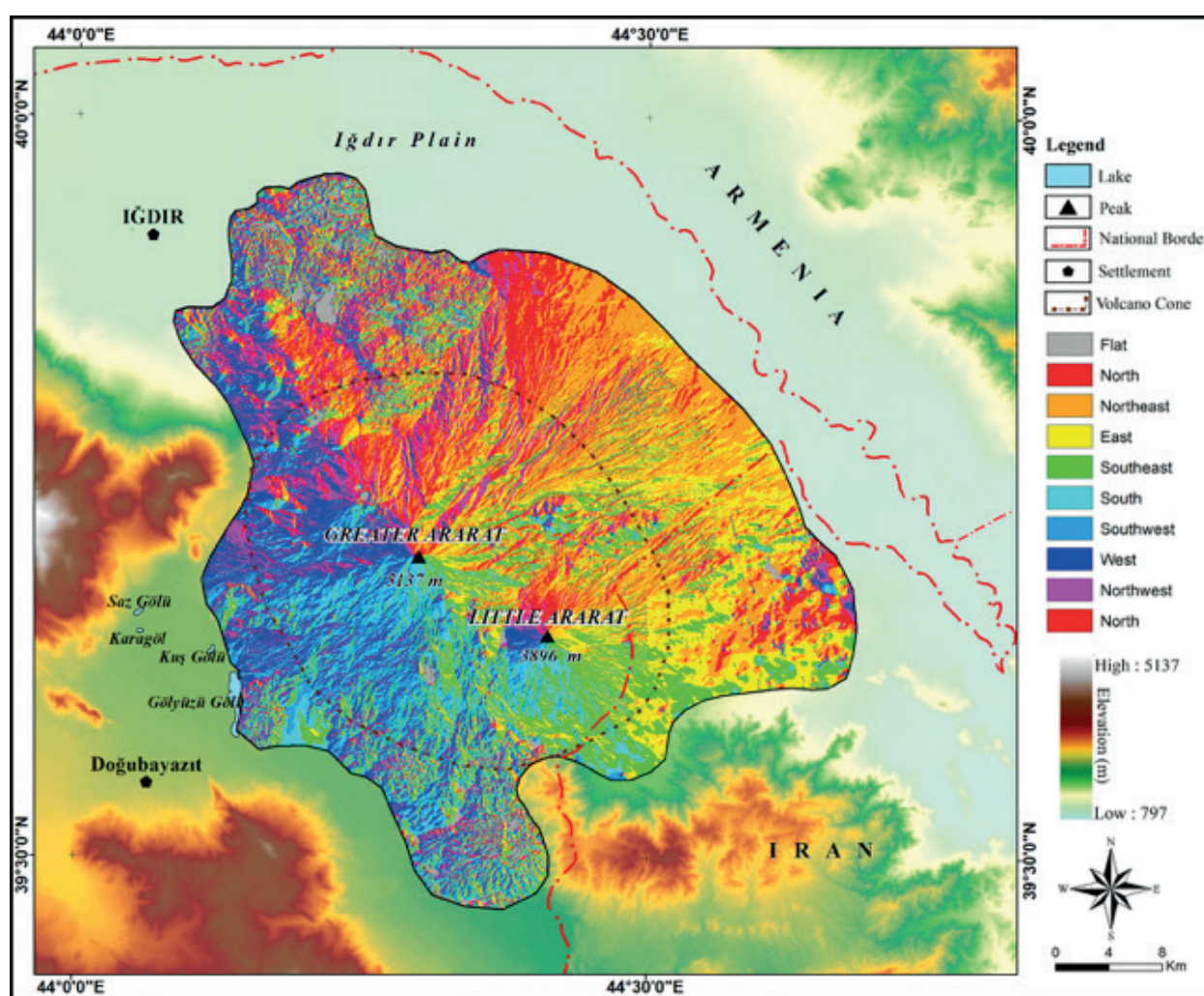


Figure 11. Aspect map of Mount Ararat.

According to the results of the analysis, the aspect is mostly concentrated in the northern sector directions and not distributed equally in all directions. The area covered by the northeast, northwest and southeast slopes of Mount Ararat is wider. The western slopes cover the smallest area. This distribution directed the glaciation on the mountain. Wider north-facing slopes have enabled the glaciers to extend further down the northern slopes.

Table 2  
Areal and percentage distribution of aspect groups in Mount Ararat

Aspect reclassification	Area (km <sup>2</sup> )	Area (%)
Flat	27	1,6
North	244	14,7
Northeast	331	19,9
East	273	16,4
Southeast	178	10,7
South	144	8,7
Southwest	145	8,7
West	163	9,8
Northwest	157	9,4
Total	1662	100,0

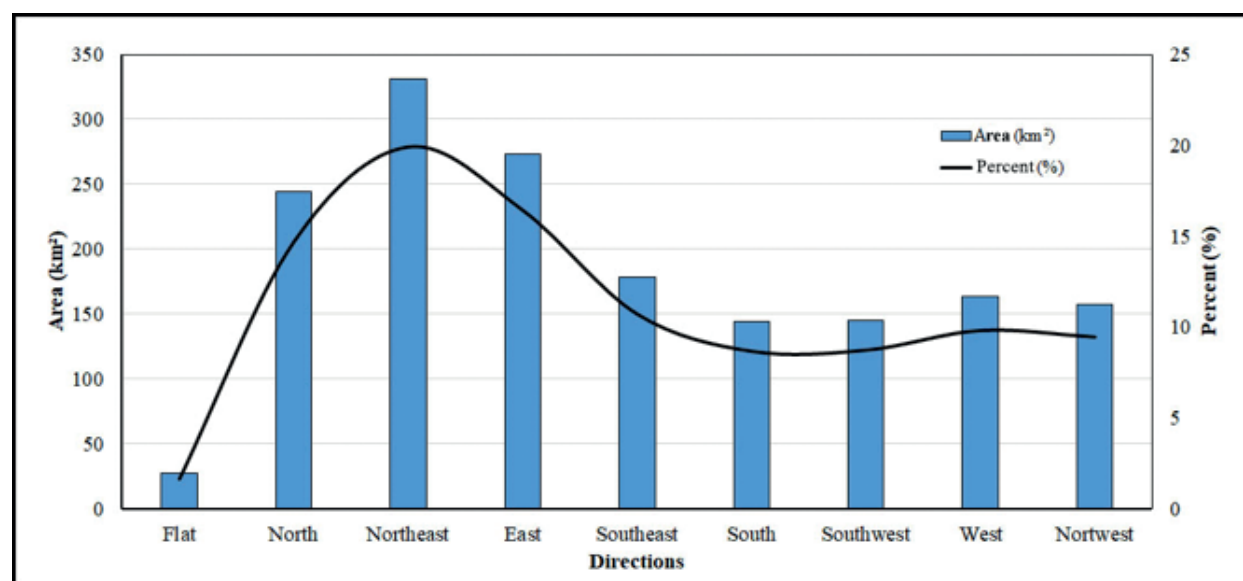


Figure 12. Areal and proportional distribution of aspect classes on Mount Ararat.

### 3.5. Relative Relief Analyses

Relative relief analyses are based on the calculation of the difference in elevation between the lowest and highest points at a specific place. In the process of morphological development, the rivers deepen their valleys by eroding backwards, towards the area of actual resource. In this way, the elevation difference between valley floors and topography surface or summits where these valleys are buried increases throughout the erosion period. Determining this difference, named relief amplitude, reveals the degree of dissected in an area (Bilgin, 2013). It gives highly reliable results in terms of the specific period of fluvial process and the effect of them in areas where these processes are prominent. According to the results of the analysis, it is possible to reach safe conclusions in volcanic lands. The morphological structure of Mount Ararat is clearly revealed through the relative relief analysis of the mountain. According to the results of the analysis, the altitude difference varies between 0-1141 m per km<sup>2</sup>. This difference in such narrow distances is related to the volcanic formation of the mountain. Relative relief values start increasing after 2500 m and reach high values at very short distances on the slopes of the cone. It is determined that the relative elevation between 3000 m and the summit of the Mountain is very high on all of the slopes on the mountain. This indicates that the Mountain summit is young and has not yet been splitted by rivers.

Greater Mount Ararat relative relief values increase after 3000 m and maximum values are observed between the summit and the elevations higher than this value. On the other hand, there are some decreases and increases in relative relief values on different points of Little Ararat. Decreases in relative relief at some points on the summit of Mount Ararat reflect the impact of glacial, stream and lava flows on this summit (Figure 13). Relative relief values are low as young lava flows cover the surface on the mountainside of both cones. The values decrease to values close to zero since the splitting disappears in the area of transition from the mountain to the plains.

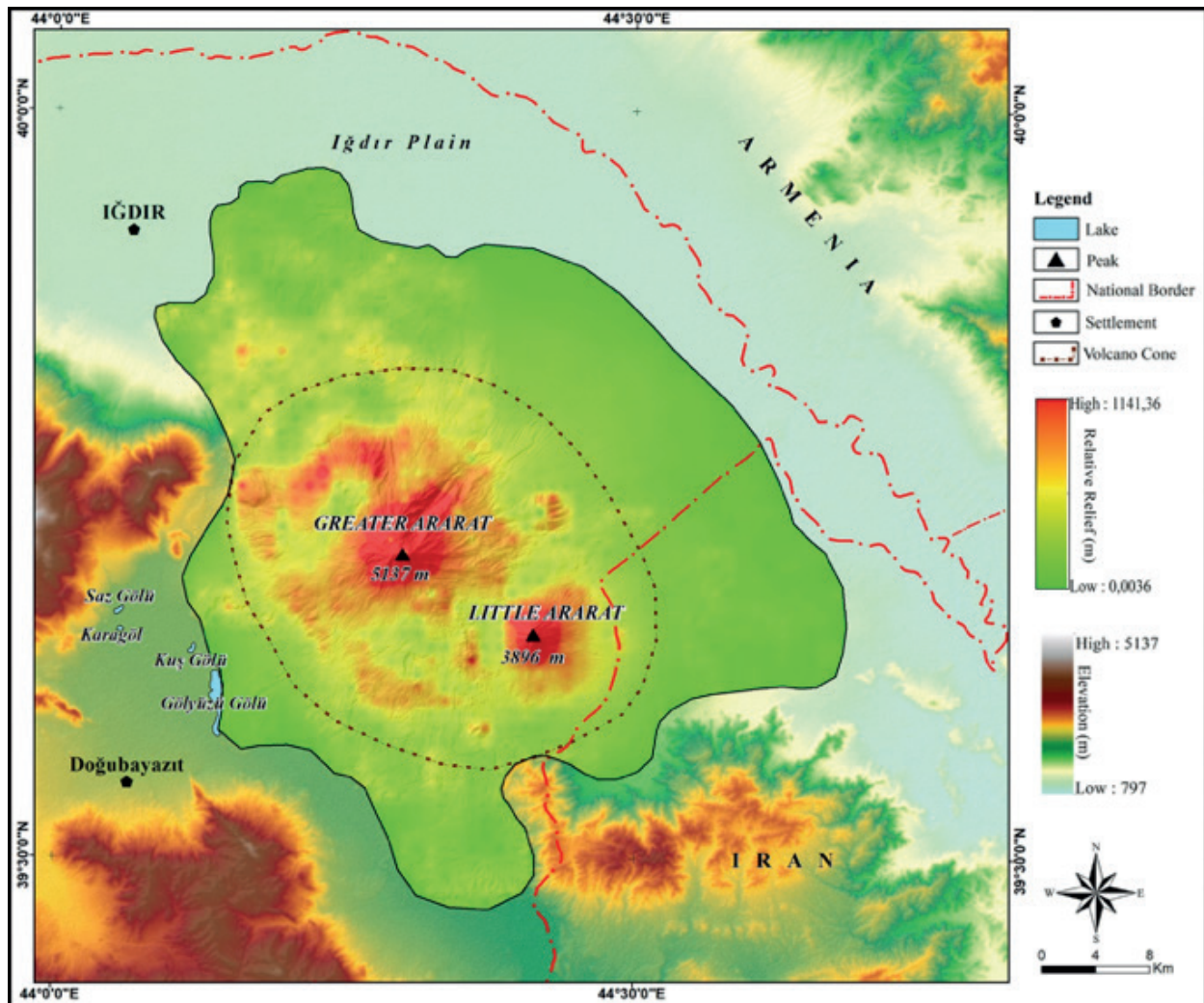


Figure 13. Relative relief map of Mount Ararat.

### 3.6. Topographic Position Index Analysis (TPI)

The topographic position index (TPI) consists of the processes of classifying and standardizing a terrain according to surface shapes and slope values, using cell values for each elevation step. At the end of the analysis, positive values indicate areas with high elevations such as mountains and hills, negative values indicate lower areas such as canyons and valleys, and index values close to zero indicate the ridges and flat areas (Jenness, 2006; Weiss, 2001). Topographic Position Index is a data analysis produced by the Digital Evaluation Model (DEM). According to the map formed by SAGA GIS software, the index values range from -18.2 to 25.1 (Figure 14). The topographic position index, which is an important source for geomorphologic maps, classifies the landforms. It determines the types of morphological variability in a specific field (Jenness, 2006; Tağıl & Jenness, 2008).

Topographic Position Index values are high at the summit of Mount Ararat because of the morphology while the values are low in the valleys and piedmond created by rivers on the slopes surrounding the cone.

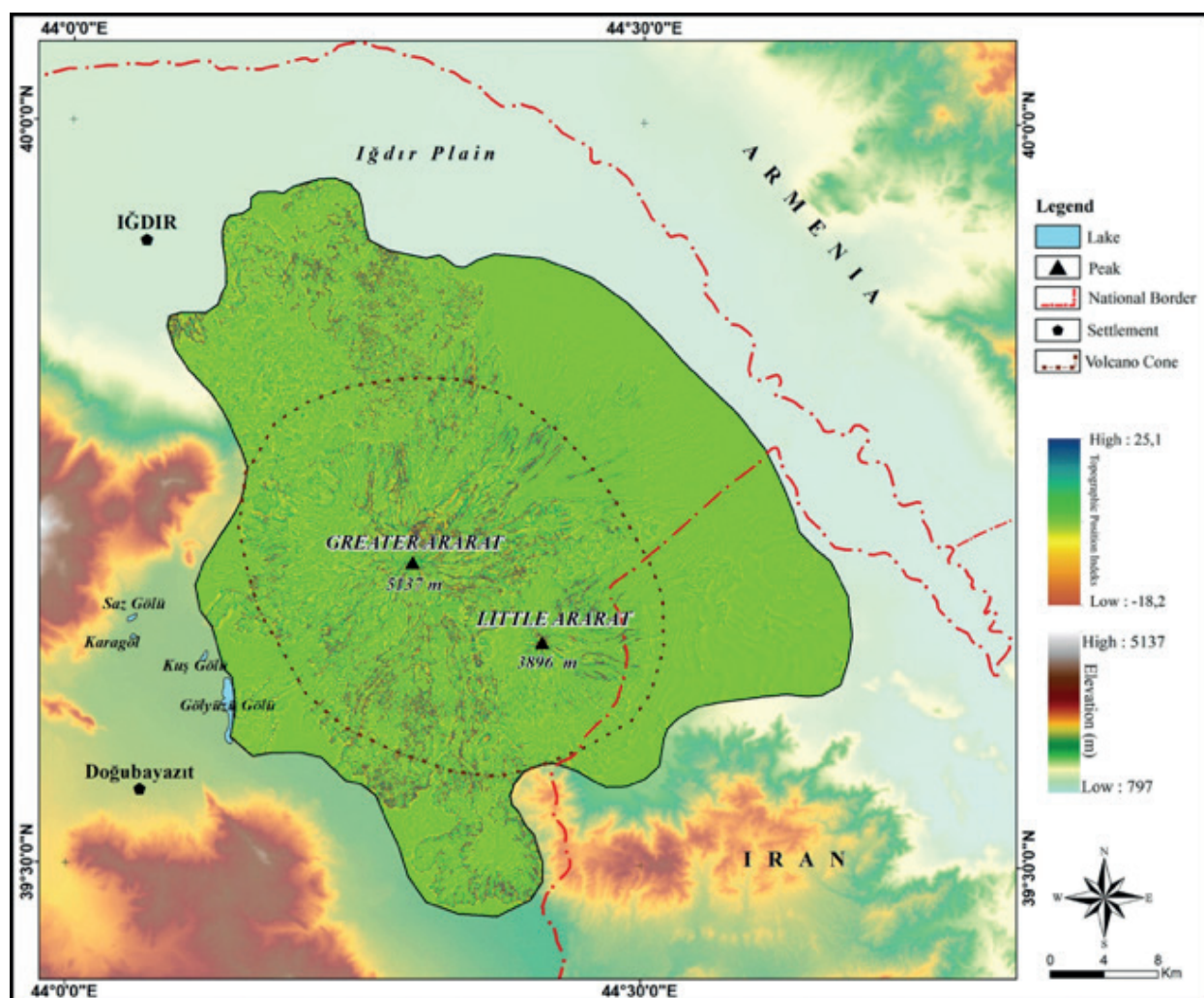


Figure 14. Topographic position index map of Mount Ararat.

According to the results map, there was a considerable amount of lava flow towards Iğdır Plain in the northwest of Mount Ararat and towards Doğubayazıt Plain in the south. On the other hand, there are other valleys on the big cone, including Cehennem creek glacial valley.

### 3.7. Topographic Curvature Analysis

This analysis shows the rate of slope change as a geomorphologic feature (Figure 15). The curvature function displays the shape or curve of the slope. A portion of a surface may be concave or convex. Curvature analysis can be used for understanding erosion and flow processes and defining basin features of a drainage basin. Profile curvature affects the acceleration and deceleration of flow, and consequently erosion and deposition. In the field, a negative value indicates that the curve is convex, a positive value indicates that the curve is concave while 0 indicates that the curve is linear (Florinsky, 1998; Shary, 1995; Smith, Goodchild, & Longley, 2012).

Positive values morphologically indicate concave shapes such as valleys and canyons while negative values indicate convex profiles such as ridges. In Mount Ararat analyses, important morphological shapes such as valley, ridge, hill, lava flows and plateau plains are seen. Geomorphology studies make an important contribution to limiting and defining shapes by combining topographic position analysis and this analysis and using both methods in narrow distances.

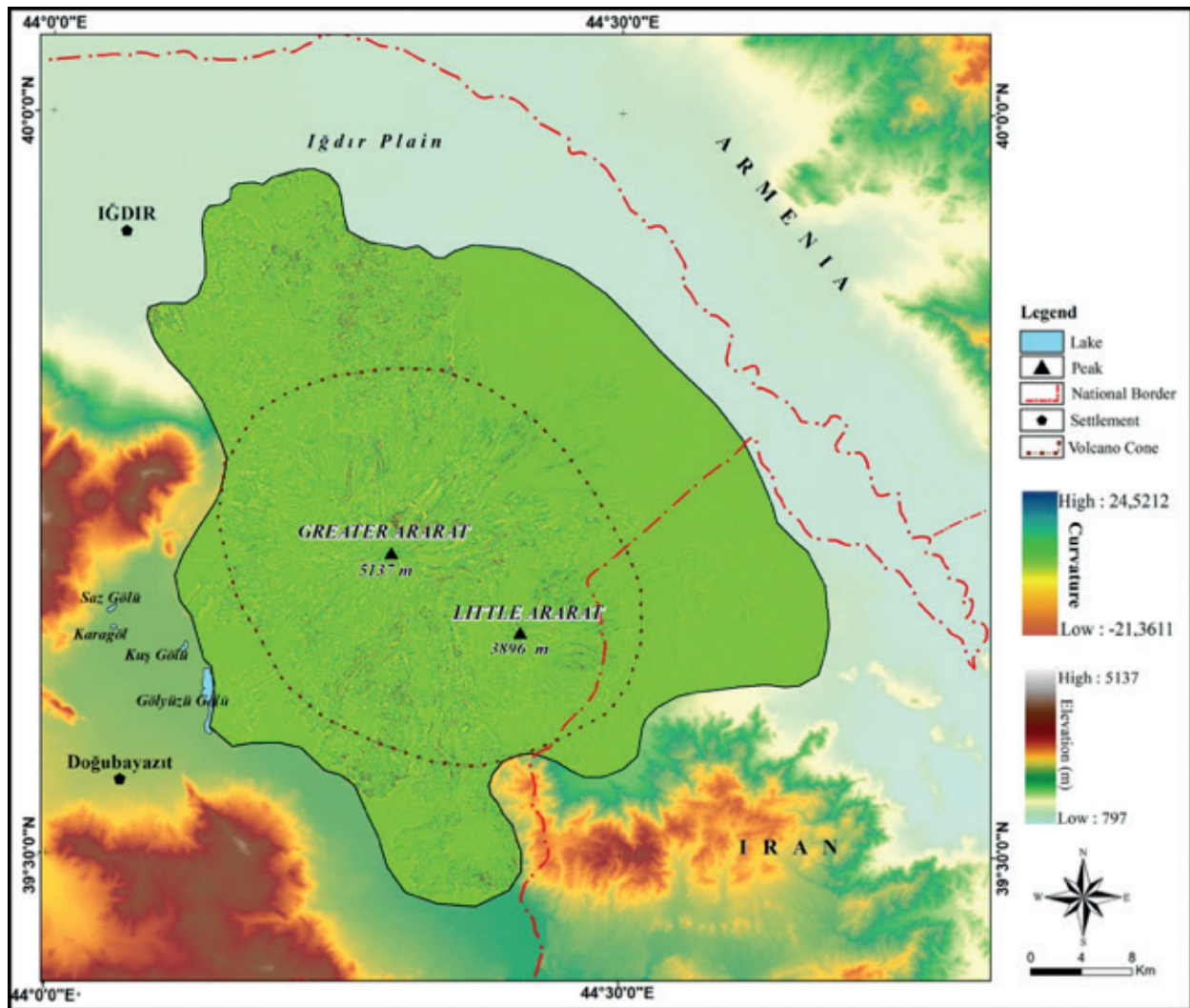


Figure 15. Topographic curvature map of Mount Ararat.

### 3.8. Terrain Ruggedness Index (TRI)

Terrain Ruggedness Index (TRI) is used to express the amount of the elevation difference between adjacent cells of a digital elevation model (DEM). It is also used as a measure of land heterogeneity (Riley et al., 1999). TRI provides new information about landslide morphology and is suggested to be specifically used for characterizing the accumulated parts of landslides (Leopold, Wolman, & Miller, 1964; Rózycka, Migoń, & Michniewicz, 2017). The topographic analysis of Mount Ararat indicates that this analysis can be used for determining volcanic cones, lava flows and other volcanic geographical formations. The volcanic formations in the northwest and south of the Mountain could be accurately determined by this method. According to this result, it can be said that terrain ruggedness index can efficiently be used for identifying landforms on volcanic areas (Figure 16).

### 3.9. Stream Order Analysis

In the first stage of the drainage basin analysis, procedures for determining the stream orders are performed. Branches of a stream are defined according to the hierarchical place of them in the basin of that stream (Leopold et al., 1964). Strahler system (Strahler, 1964) classifies the smallest tributary as the first stream order. The junction of the two first tributary streams is called the 2nd stream order and one upper upstream is called the 3rd stream order. When different sequences (streams) are combined in this way, the greater sequences (streams) form the upper order while the mainstream forms the stream segment of the highest order (Strahler, 1964). The border based on Mount Ararat distribution volcanic material covers 1662 km<sup>2</sup>. The rivers in this area have a radial drainage network and the main flows are on the sixth order. It is determined that there are 6 main flows and 19,041 smaller flows on Mountain Ararat (Figure 17).

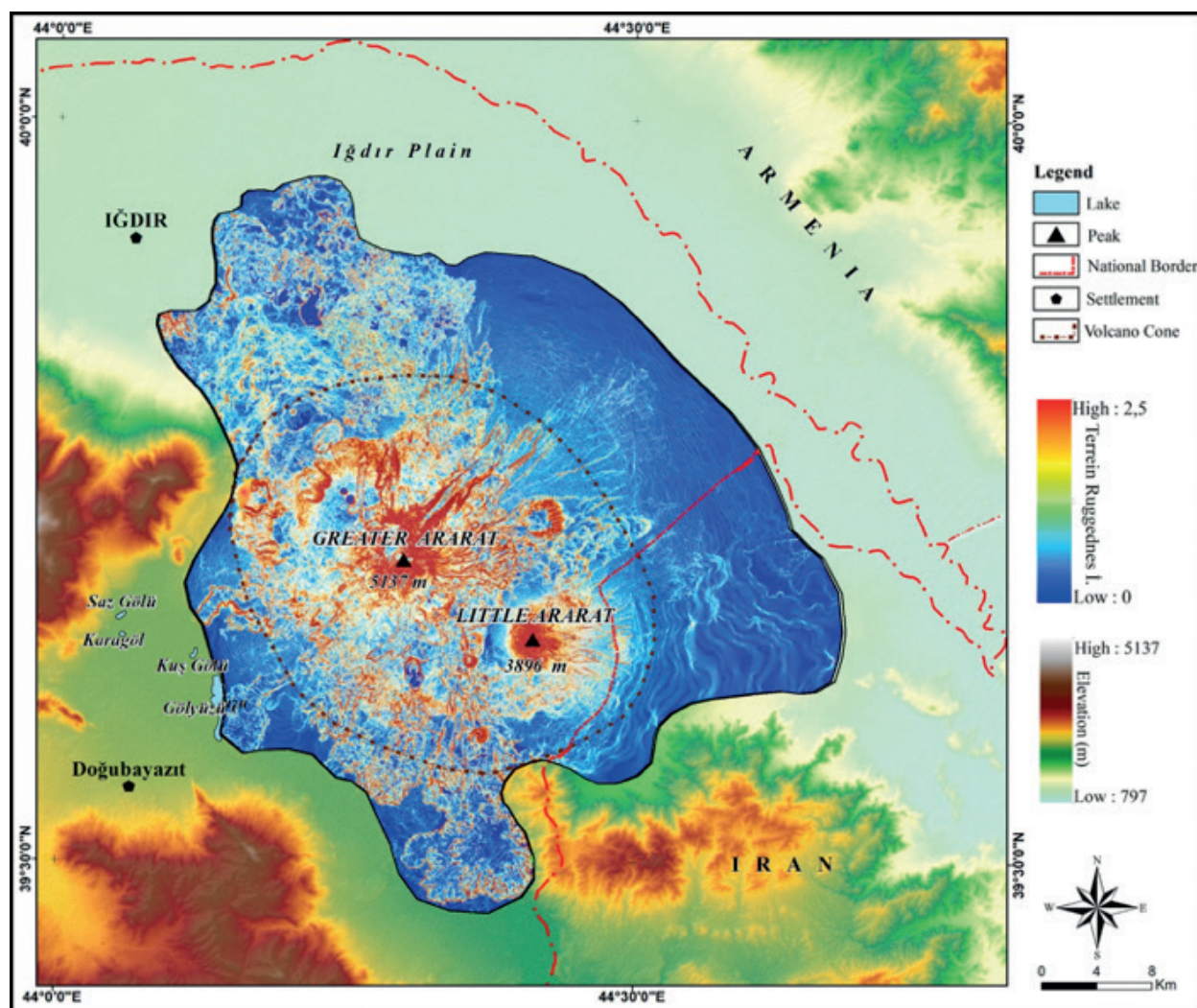


Figure 16. Terrain ruggedness map of Mount Ararat.

According to the analysis results, 1st order streams involve 14.483 flow sections while the 2nd order streams involve 2.337 flow sections. The 6th order streams involve the lowest number of flow sections (8). It is observed that there is a decrease in the stream frequency in line with the increase in the stream order. The flows in the first-order account for 52.3% and the flows in the second-order account for 27.5% of the total number of flows. 1st and 2nd order streams make up more than 75% of the area (Table 3). The 3rd and 4th order streams account for 18%, while the 5th and 6th order streams account for 2.2% of the streams. All of these results are specific to young volcanic cones.

Table 3

Number, length and order ratio of streams in Mount Ararat

Stream Order	Stream Number	Stream Length (km)	Stream Order (%)
1	14.483	2638,8	52,3
2	2.337	1387,4	27,5
3	1.227	588,1	11,7
4	752	319,3	6,3
5	234	107,8	2,1
6	8	5,6	0,1
Total	19.041	5046.9	100

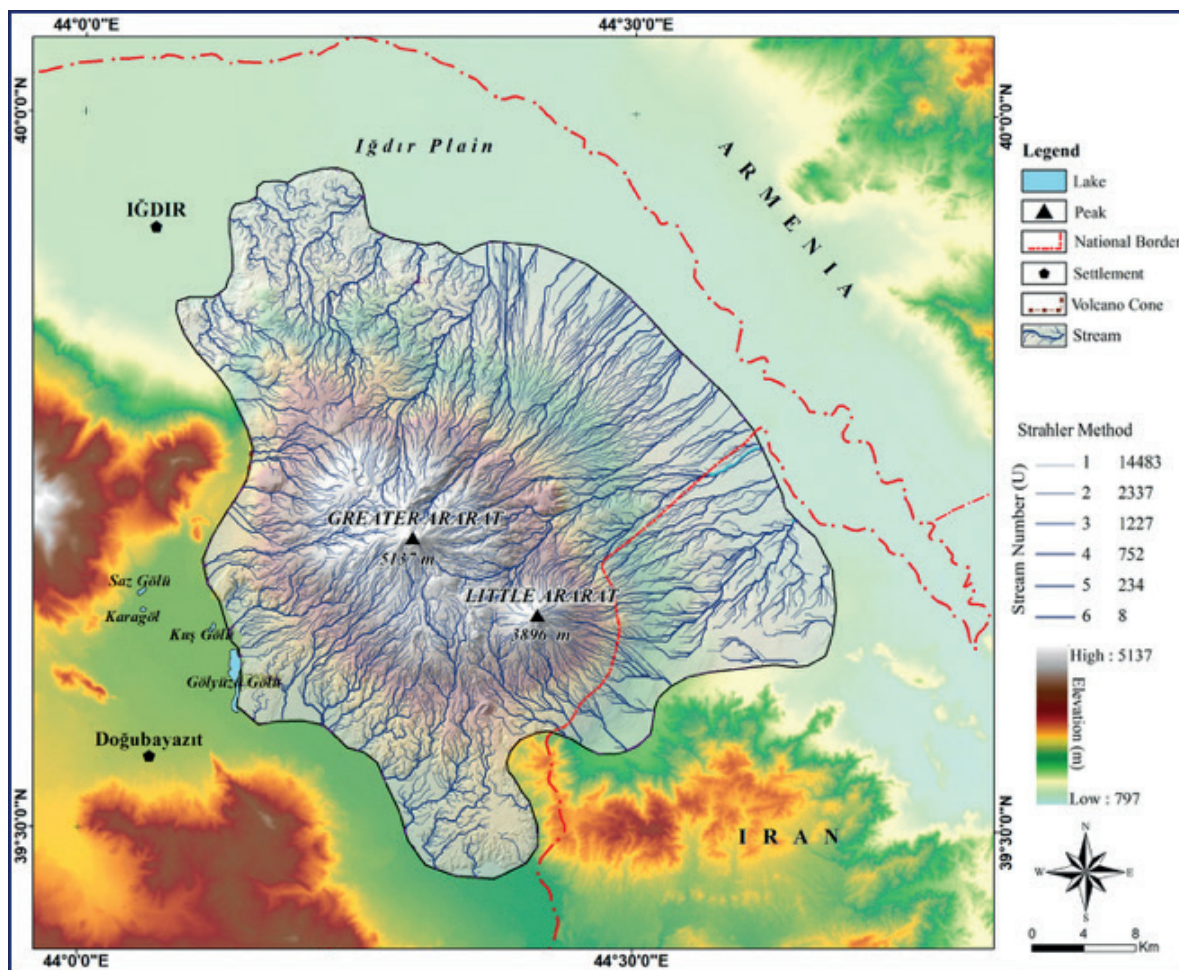


Figure 17. Stream order map of Mount Ararat.

### 3.10. Drainage Density Analysis

It is known that drainage density varies with the agents such as climate, vegetation, geomorphology, soil and rock characteristics (Kelson & Wells, 1989; Moglen, Eltahir, & Bras, 1998). In this method, values between 0 and 2 indicate low density, values between 2 and 2.5 indicate medium, values between 2.5 and 3 indicate high, and the values between 3 and higher indicate high drainage density (Malik, Bhat, & Kuchay, 2011). According to the analysis results, the drainage density is high in 18% and very high in 82% of the river basins on Mount Ararat. According to these results, river activity was very dominant in the formation of the Mountain. The morphological structure of the mountain and the ice cap glacier at the summit are effective in this very high drainage density level. On the other hand, these results prove the young and high volcano cone structure of the mountain. The northeast mountainside, where the drainage density is very high, corresponding to the wide fans and show the efficacy of torrent streams (Figure 18; Table 4).

Table 4  
Drainage Density and Percentage Values of Mount Ararat

Drainage Density (Dd)	Sub-basin	Percentage (%)
Low (0-2)	0	0
Medium (2-2,5)	0	0
High (2,5-3)	11	18,0
Very High (3- +)	50	82,0
Total	61	100

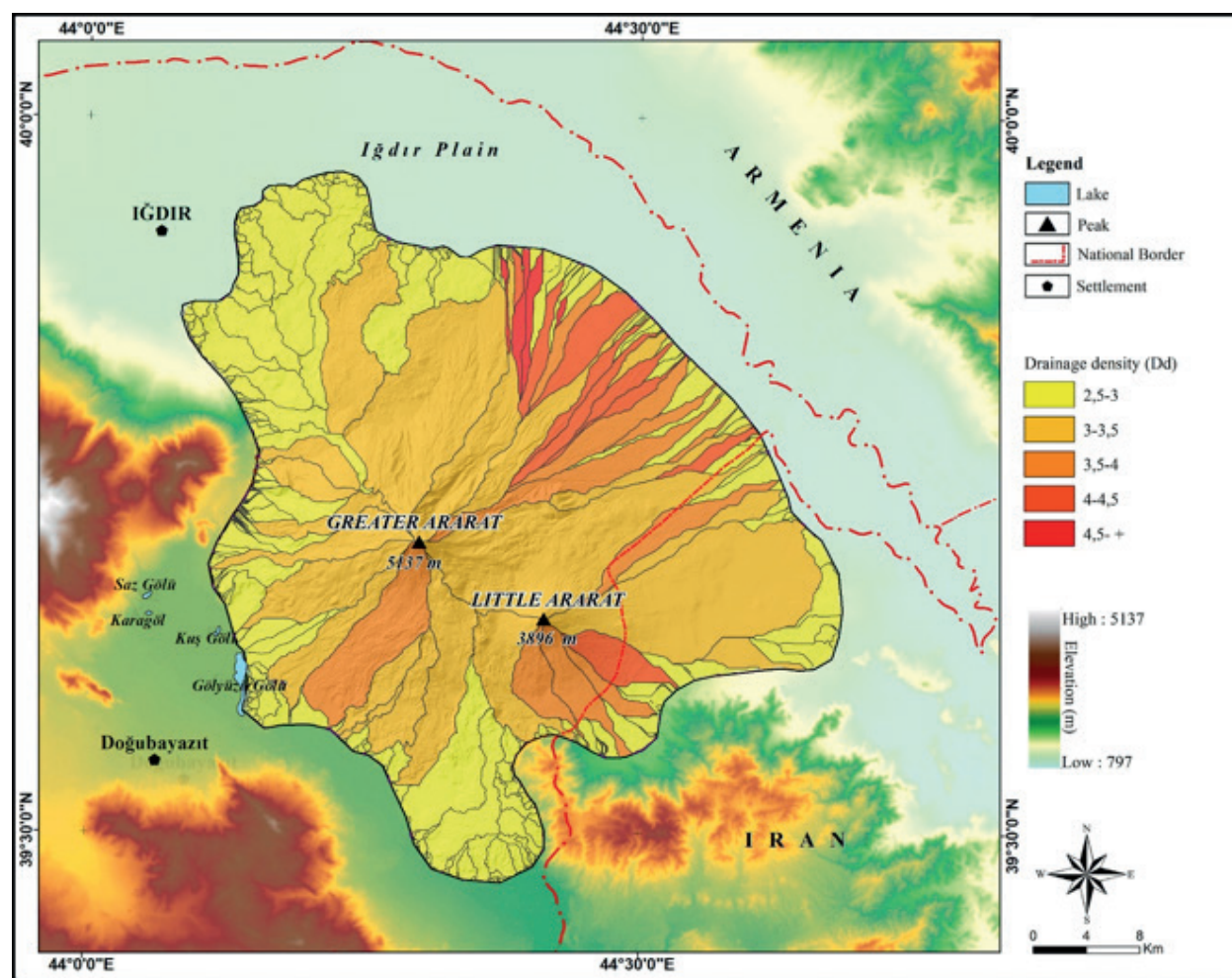


Figure 18. Drainage density map of Mount Ararat

### 3.11. Hypsometric Curve and Integral

The hypsometric curve shows the distribution of height in a basin and gives information about geological and geomorphological stages of basin development and basin erosion (Garg, 1983; Strahler, 1952b). The hypsometric integral provides data about geomorphological development stages in an area. Integral values vary between 0-1 and the proximity to 0 represents the mature basin and the proximity to 1 represents the young basin (Keller & Pinter, 2002; Strahler, 1952b). For the hypsometric integral analysis of Mount Ararat, the area in the boundary of the volcano cone was evaluated and the integral value was calculated as 0.28. When other morphometric analysis results are compared with this analysis, the presence of wide plains (except cone) on Mount Ararat is observed. According to this value, most of the analysed areas are mature basins. While the slopes of the cone higher than 2500 m mean young topography, there are wide volcanic plains below this elevation. Considering this topographic situation, it can be said that the result is correct (Figure 19).

## 4. Conclusion

Mount Ararat is the highest mountain in Türkiye. Apart from this feature, it is also important for being an existing ice-capped volcano. It is a strato-volcano formed on a circular area with an average diameter of 30-35 km. The mountain consists of two volcanic cones above an altitude of 2500 m. The decrease in the distance between the elevation ranges according to elevation map, the increase in the slope values at the summit and the relative relief difference of 0-1141 m per km<sup>2</sup> show the morphological feature of the mountain in the shape of cone. All analyses except that of aspect showing the extent support this result. The volcano cones and the surrounding flats are noticeably separated according to the slope,

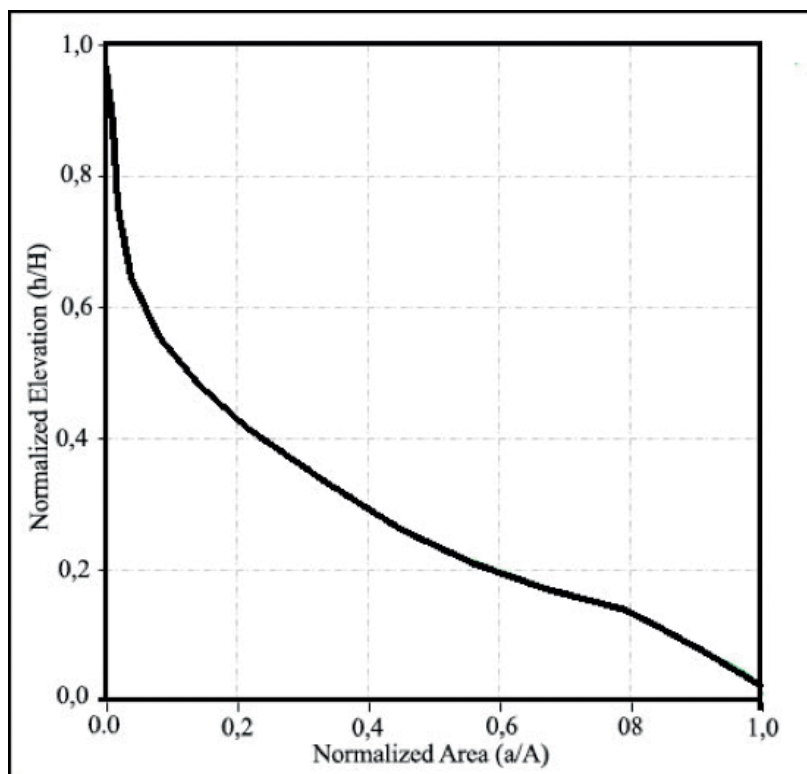


Figure 19. Hypsometric curves of Mount Ararat (Drawn with the Calhypo plugin (Pérez-Peña et al., 2009))

relative relief, topographic position, and topographic curvature analyses. Topographic position and topographic curvature analysis demonstrates all of the main geomorphologic units on the mountainous mass. Terrain ruggedness analysis is a reliable technique for observing and analyzing landslides; it has been determined that the method is also reliable for analyzing volcanic areas. According to the data obtained through this analysis, the boundaries of the lava flows are particularly very clear. The radiant structure of the drainage specific to the volcano cones is evident in the stream order and drainage density analyses. Morphometric analyses helps conducting detailed geomorphology studies in extremely wide, volcanic terrain and topographically rough areas like Mount Ararat. It is clear that these analyses will provide great, reliable support to accurate identification of some morphological units that are not very prominent in the field.

### Acknowledgement

Part of this study was presented at the Fourth International Symposium on Mount Ararat and Noah's Ark.

### Author Contributions

Vedat Avci: He has planned the study, performed 10 analyses and created the figures and texts under the headings related to these analyses.

Murat Sunkar: He has planned the study, written the summary, introduction and conclusion sections, checked the figures prepared according to the results of analyses and made the arrangements.

Ahmet Toprak: He has contributed to the method section, performed 5 analyses and created the texts under the headings related to these analyses.

### Conflicts of Interest

The authors declare no conflict of interest.

## References

- ArcGIS Desktop Help. (2022). Environmental Systems Research Institute.
- Ardel, A. (1968). *Jeomorfolojinin Prensipleri, Fasikül I.* İstanbul: İstanbul University Institute of Geography Publication.
- Arkel, N. van. (1973). Die Gegenwärtige Vergletscherung des Ararat (The present-day glaciation of Ararat). *Zeitschrift Für Gletscherkunde Und Glazialgeologie*, (9), 89–103.
- ASF. (2019). *Alaska Satellite Facility Data Search User Manual*. Retrieved from: <https://search.asf.alaska.edu/>
- Atalay, İ. (2017). *Türkiye Jeomorfolojisi*. İzmir: Meta Printing Services.
- Avcı, V., & Sunkar, M. (2015). Morphometric Analyses of Aksu Stream And Batlama Creek Watersheds That Caused Flood and Overflows in Giresun. *Journal of Geography*, (30), 91–119.
- Avcı, V., & Sunkar, M. (2018). Morphometric Analysis of Pazarsuyu, İncüvez, Kara and Bulancak Streams Which Cause Flood and Overflow Events in Bulancak (Giresun). *Firat University Journal of Social Sciences*, 28 (2), 15–41. Doi: <https://doi.org/10.18069/firatsbed.460907>
- Avcı, V., Sunkar, M., & Toprak, A. (2018). Ağrı Dağı'nın (Ararat) Morfometrik Analizleri. In O. Belli, F. Kaya, İ. Özgül, & V. E. Belli (Eds.), *The Fourth International Mount Ararat And Noah's Ark Symposium (pp. 124-132.)*, Ağrı, Turkey.
- Azzoni, R. S., Zerboni, A., Pelfini, M., Garzonio, C. A., Cioni, R., Meraldi, E., & Diolaiuti, G. A. (2017). Geomorphology of Mount Ararat/Ağrı Dağı (Ağrı Dağı Milli Parkı, Eastern Anatolia, Turkey). *Journal of Maps*, 13(2), 182–190. Doi: <https://doi.org/10.1080/17445647.2017.1279084>
- Azzoni, R. S., Fugazza, D., Garzonio, C. A., Nicoll, K., Diolaiuti, G. A., Pelfini, M., & Zerboni, A. (2019). Geomorphological effects of the 1840 Ahora Gorge catastrophe on Mount Ararat (Eastern Turkey). *Geomorphology*, (332), 10-21. Doi: <https://doi.org/10.1016/j.geomorph.2019.02.0011>
- Bilgin, T. (2013). *Kartoğrafya II*. İstanbul: Filiz Kitabevi.
- Blumenthal, M. M. (1956). Die Vergletscherung des Ararat (Nordöstliche Türkei). *Geographica Helvetica*, 11(4), 263–264.
- Blumenthal, M. M. (1958). Vom Ağrı Dag (Ararat) zum Kaçkar Dag. Bergfahrten in nordost anatolischen Glanzlanden (From Mount Ararat to Mount Kaçkar Mountain trip in the frontier region of northeastern Anatolia). *Die Alpen*, (34), 125–137.
- Çiner, A. (2003). Recent glaciers and late quaternary glacial deposits of Turkey. *Geological Bulletin of Turkey*, 46(1), 56–78.
- Erginal, A. E., & Cürebal, İ. (2007). Soldere Havzasının Jeomorfolojik Özelliklerine Morfometrik Yaklaşım: Jeomorfik İndisler İle Bir Uygulama. *Selçuk Üniversitesi Sosyal Bilimler Enstitüsü Dergisi*, (17), 203–210.
- Erinç, S. (1953). *Doğu Anadolu Coğrafyası*. İstanbul: İstanbul University Geography Institute Publication
- Erol, O. (1993). Ayrıntılı jeomorfoloji haritaları çizim yöntemi. *İstanbul Üniversitesi Deniz Bilimleri ve Coğrafya Enstitüsü Bülteni*, (10), 19–37.
- Florinsky, I. V. (1998). Accuracy of local topographic variables derived from digital elevation models. *International Journal of Geographical Information Science*, 12 (1), 47-62. Doi: <https://doi.org/10.1080/136588198242003>
- Garg, S. K. (1983). *Geology-The science of the earth*. New Delhi: Khanna Publication
- General Directorate Mapping (GDM). (2004). 1/25.000 Ölçekli Topoğrafya Haritaları I52 ve I 53 paftaları. Ankara.
- Güner, Y., & Şaroğlu, F. (1987). Doğu Anadolu'da Kuvaterner volkanizması ve jeotermal enerji açısından önemi. *Türkiye 7. Petrol Kongresi* (371-383). Ankara, Turkey.

- Horton, R. E. (1932). Drainage-basin characteristics. *Eos, Transactions American Geophysical Union*, 13(1), 350–361. Doi: <https://doi.org/10.1029/TR013i001p00350>
- Horton, R. E. (1945). Erosional development of streams and their drainage basins; hydrophysical approach to quantitative morphology. *Geological Society of America Bulletin*, 56(3), 275–370. Doi: [https://doi.org/10.1130/0016-7606\(1945\)56\[275:EDOSAT\]2.0.CO;2](https://doi.org/10.1130/0016-7606(1945)56[275:EDOSAT]2.0.CO;2)
- Imhof, B. (1956). Der Ararat. *Die Alpen*, 32(1), 1–14.
- Jenness, J. (2006). Topographic Position Index extension for ArcView 3. X, v. 1.2., Jenness Enterprises.
- Kaya, F. (2017). *Ağrı Dağı*. Ağrı: Republic of Turkey Agri Governorship Provincial Culture and Tourism Directorate Publications.
- Keller, E. A., & Pinter, N. (2002). *Active tectonics: Earthquakes, uplift, and landscape*. New Jersey: Prentice-Hall.
- Kelson, K. I., & Wells, S. G. (1989). Geologic influences on fluvial hydrology and bedload transport in small mountainous watersheds, northern New Mexico, USA. *Earth Surface Processes and Landforms*, 14 (8), 671–690. Doi: <https://doi.org/10.1002/esp.3290140803>
- Leopold, L. B., Wolman, M. G., & Miller, J. P. (1964). *Fluvial processes in geomorphology*. New York: Dover Publications.
- Malik, M. I., Bhat, M. S., & Kuchay, N. A. (2011). Watershed based drainage morphometric analysis of Lidder catchment in Kashmir valley using geographical information system. *Recent Research in Science and Technology*, 3(4), 118–126. Doi: <https://doi.org/10.25081/rrst.2017.9.3355>
- Moglen, G. E., Eltahir, E. A. B., & Bras, R. L. (1998). On the sensitivity of drainage density to climate change. *Water Resources Research*, (34), 855–862. Doi: <https://doi.org/10.1029/97WR02709>
- Özşahin, E. (2015). Geomorphometric Features Of Hoşkoy River Basin (Tekirdag). *International Journal of Social Science*, (33), 99–120. Doi: <http://dx.doi.org/10.9761/JASSS2678>
- Pérez-Peña, J. V., Azañón, J. M., & Azor, A. (2009). CalHypso: An ArcGIS extension to calculate hypsometric curves and their statistical moments. Applications to drainage basin analysis in SE Spain. *Computers & Geosciences*, 35(6), 1214-1223. Doi: <https://doi.org/10.1016/j.cageo.2008.06.006>
- Rich, J. L. (1916). A graphical method of determining the average inclination of a land surface from a contour map. *Transaction Illinois Academy of Science*, (9), 196–199.
- Riley, S. J., DeGloria, S. D., & Elliot, R. (1999). Index that quantifies topographic heterogeneity. *Intermountain Journal of Sciences*, 5(1–4), 23–27.
- Rózycka, M., Migoń, P., & Michniewicz, A. (2017). Topographic wetness index and terrain ruggedness index in geomorphic characterisation of landslide terrains, on examples from the Sudetes, SW Poland. *Zeitschrift Für Geomorphologie, Supplementary Issues*, (61), 61–80. Doi: [https://doi.org/10.1127/zfg\\_suppl/2016/0328](https://doi.org/10.1127/zfg_suppl/2016/0328)
- Sarıkaya, M. A. (2012). Recession of the ice cap on Mount Ağrı (Ararat), Turkey, from 1976 to 2011 and its climatic significance. *Journal of Asian Earth Sciences*, (46), 190–194. Doi: <https://doi.org/10.1016/j.jseas.2011.12.009>
- Schumm, S. A. (1956). Evolution of drainage systems and slopes in badlands at Perth Amboy, New Jersey. *Geological Society of America Bulletin*, 67(5), 597–646. Doi: [https://doi.org/10.1130/0016-7606\(1956\)67\[597:EODSAS\]2.0.CO;2](https://doi.org/10.1130/0016-7606(1956)67[597:EODSAS]2.0.CO;2)
- Shary, P. A. (1995). Land surface in gravity points classification by a complete system of curvatures. *Mathematical Geology*, 27(3), 373–390. Doi: <https://doi.org/10.1007/BF02084608>
- Smith, K. G. (1950). Standards for grading texture of erosional topography. *American Journal of Science*, 248 (9), 655–668. Doi: <https://doi.org/10.2475/ajs.248.9.655>
- Smith, M. J., Goodchild, M. F., & Longley, P. A. (2012). *Geospatial Analysis: A Comprehensive Guide to Principles, Techniques and Software Tools*. Leicester: Matador Publication. Retrieved from: <https://>

- scholar.google.com/scholar?hl=tr&as\_sdt=0%2C5&q=Geospatial+analysis%3A+A+comprehensive+guide%2C+Electronic+book.&btnG=
- Strahler, A. N. (1952a). Dynamic basis of geomorphology. *Geological Society of America Bulletin*, 63 (9), 923–938. Doi: [https://doi.org/10.1130/0016-7606\(1952\)63\[923:DBOG\]2.0.CO;2](https://doi.org/10.1130/0016-7606(1952)63[923:DBOG]2.0.CO;2)
- Strahler, A. N. (1952b). Hypsometric Analysis of Erosional Topography. *Bull. Geol. Soc. Am.* (63), Doi: [https://doi.org/10.1130/0016-7606\(1952\)63\[1117:HAAOET\]2.0.CO;2](https://doi.org/10.1130/0016-7606(1952)63[1117:HAAOET]2.0.CO;2)
- Strahler, A. N. (1964). Quantitative geomorphology of drainage basins and channel net work. New York: In Chow, V.T. (ed.) *Handbook of Applied Hydrology*, McGraw-Hill, 4–76.
- Şahin, C. (2011). *Türkiye Fiziki Coğrafyası* (Extended 4th Edition). Ankara: Daytime Education and Publishing.
- Şenel, M., & Ercan, T. (2002). *1/500.000 Ölçekli Türkiye Jeoloji Haritaları, Van Paftası*. Ankara: Maden Tetkik ve Arama Genel Müdürlüğü.
- Tağıl, Ş., & Jenness, J. (2008). GIS-based automated landform classification and topographic, landcover and geologic attributes of landforms around the Yazoren Polje, Turkey. *Journal of Applied Sciences*, 8(6). Doi: [10.3923/jas.2008.910.921](https://doi.org/10.3923/jas.2008.910.921)
- Topuz, M., & Karabulut, M. (2016). Geomorphometric Analysis Of Limonlu And Alata Watersheds (Erdemli, Mersin, Turkey). *Electronic Turkish Studies*, 11(2), 1231-1250. Doi: <http://dx.doi.org/10.7827/TurkishStudies.9165>
- Turoğlu, H. (2011). *Coğrafi Bilgi Sistemlerinin Temel Esasları*. İstanbul: Çantay Kitabevi.
- Türkecan, A. (2017). Türkiye'nin Doğu Bölgelerinde Gözlenen Kuvaterner Yaşlı Volkanik Etkinlikleri. *Doğal Kaynaklar ve Ekonomi Bülteni*, (22), 63-78.
- Türkunal, S. (1980). *Doğu ve Güneydoğu Anadolu'nun Jeolojisi*. Ankara: Chamber of Geological Engineers Publication.
- Weiss, A. (2001). Topographic position and landforms analysis. *ESRI User Conference*. San Diego, USA. Retrieved from: [http://www.jennessent.com/downloads/tpi-postertnc\\_18x22.pdf](http://www.jennessent.com/downloads/tpi-postertnc_18x22.pdf)
- Wilson, J. P., & Gallant, J. C. (2000). *Terrain analysis: Principles and Applications*. New York: John Wiley & Sons.